8. Materials and methods are available as supporting material on *Science* Online.
9. D. R. Piperno, D. M. Pearsall, *The Origins of Agriculture in the Lowland Neotropics* (Academic Press, San Diego, CA, 1998).
10. T. C. Andres, R. W. Robinson, in *Cucurbitaceae 2002*, D. N. Maynard, Ed. (ASHS Press, Alexandria, VA, 2002), pp. 95–99.
11. M. Nee, *Econ. Bot.* **44**, 56 (1990).
12. Despite extensive searches, no other wild *Cucurbita* has been found in Ecuador (*10*, *11*). *C. ecuadorensis* is believed to have been at least semi-domesticated and used more commonly in the past than it is at the present time (*10*, *11*). Many free-living populations, which are common in dry forest and along streams and road banks, have small (~8 to 10 cm long) and bitter fruits. Vines found today in house gardens, where they are grown or maintained and consumed by humans or more commonly fed to domestic animals, have fruits with sizes of domesticated species (from 12 to 14 cm long and 12 to 18 cm in diameter) and other domesticated characteristics, such as nonbitter flesh, nonlignified rinds, and considerable variability in color and pattern (*10*).
13. S. R. Bozarth, *Am. Antiq.* **52**, 607 (1987).
14. D. R. Piperno, I. Holst, L. Wessel-Beaver, T. C. Andres, *Proc. Natl. Acad. Sci. U.S.A.* **99**, 10923 (2002).
15. Phytoliths are placed in fruit rinds in such a way that they straddle the interface between the hypodermis and the outermost stone (lignified) cells. Phytolith thickness is greatly influenced by how large the stone cells are. Domesticated fruits make longer and larger stone cells than do wild fruits, hence phytolith thickness is also a sensitive indicator of domestication (*14*).
16. O. I. Sanjur, D. R. Piperno, T. C. Andres, L. Wessel-Beaver, *Proc. Natl. Acad. Sci. U.S.A.* **99**, 535 (2002).
17. D. W. Lathrap, D. Collier, H. Chandra, *Ancient Ecuador: Culture, Clay, and Creativity, 3000-300 B.C.* (Field Museum of Natural History, Chicago, IL, 1975).
18. D. M. Pearsall, in *Dumbarton Oaks Conference on the Ecuadorian Formative*, J. S. Raymond, R. Burger, Eds. (Dumbarton Oaks, Washington, DC, 1996), pp. 213–257.
19. J. R. Harlan, *Science* **174**, 468 (1971).
20. Supported by the Smithsonian Tropical Research Institute and the Museo Antropológico, Banco Central del Ecuador (Guayaquil).

Supporting Online Material
www.sciencemag.org/cgi/content/full/299/5609/1054/DC1
Materials and Methods
Fig. S1
Table S1

11 November 2002; accepted 26 December 2002

Control of Regulatory T Cell Development by the Transcription Factor *Foxp3*

Shohei Hori,[1] Takashi Nomura,[2] Shimon Sakaguchi[1,2]*

Regulatory T cells engage in the maintenance of immunological self-tolerance by actively suppressing self-reactive lymphocytes. Little is known, however, about the molecular mechanism of their development. Here we show that *Foxp3*, which encodes a transcription factor that is genetically defective in an autoimmune and inflammatory syndrome in humans and mice, is specifically expressed in naturally arising CD4$^+$ regulatory T cells. Furthermore, retroviral gene transfer of *Foxp3* converts naïve T cells toward a regulatory T cell phenotype similar to that of naturally occurring CD4$^+$ regulatory T cells. Thus, *Foxp3* is a key regulatory gene for the development of regulatory T cells.

To maintain immunological unresponsiveness to self-constituents (i.e., self-tolerance), potentially hazardous self-reactive lymphocytes are eliminated or inactivated during their development (*1*). Activation and expansion of self-reactive T lymphocytes that have escaped thymic clonal deletion is actively suppressed in the periphery by naturally occurring CD4$^+$ regulatory T cells (T_R), the majority of which constitutively express CD25 [interleukin (IL)-2 receptor α-chain] (*2*–*6*). CD25$^+$CD4$^+$ T_R cells are at least in part produced by the thymus as a functionally mature T cell subpopulation (*7*, *8*), and their reduction or functional alteration in rodents leads to the spontaneous development of various organ-specific autoimmune diseases including autoimmune thyroiditis, gastritis, and type 1 diabetes (*6*–*9*). T_R cells also appear to maintain a balanced response to environmental antigens, preventing inflammatory bowel disease (IBD) and allergy in rodents (*10*, *11*).

Several studies have provided findings that offer clues to the potential pathway by which T_R cells develop. Similar multiorgan autoimmune diseases, allergy, and IBD develop in the X-linked recessive disease, IPEX (immune dysregulation, polyendocrinopathy, enteropathy, X-linked syndrome) or XLAAD (X-linked autoimmunity-allergic dysregulation syndrome) (*12*). A mouse mutant strain,

[1]Laboratory of Immunopathology, Research Center for Allergy and Immunology, Institute for Physical and Chemical Research, Yokohama 230–0045, Japan. [2]Department of Experimental Pathology, Institute for Frontier Medical Sciences, Kyoto University, Kyoto 606–8507, Japan.

*To whom correspondence should be addressed. E-mail: shimon@frontier.kyoto-u.ac.jp

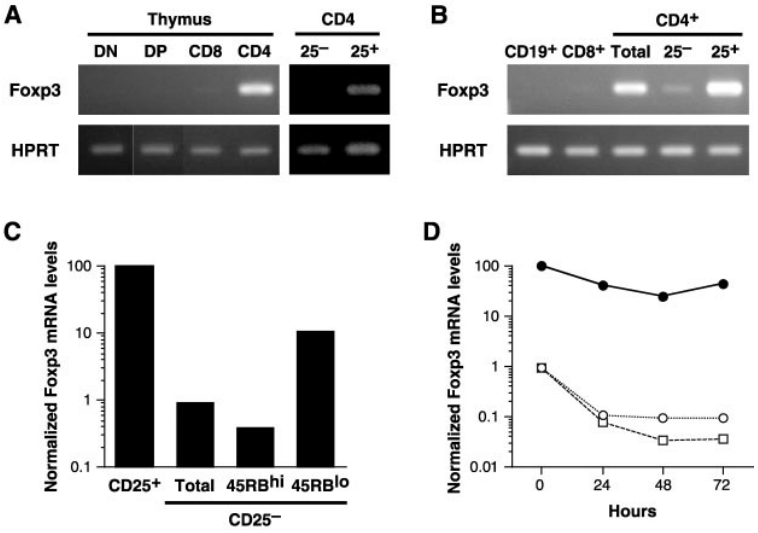

Fig. 1. Expression of *Foxp3* in a subpopulation of CD4$^+$ T cells in the thymus and periphery. (**A**) BALB/c thymocytes were sorted into CD4$^-$CD8$^-$ (DN), CD4$^+$CD8$^+$ (DP), CD4$^-$8$^+$ (CD8) or CD4$^+$8$^-$ (CD4) cells (left). CD4$^+$8$^-$ thymocytes were further separated into CD25$^+$ or CD25$^-$ cells (right). cDNA from each population was subjected to nonsaturating PCR using *Foxp3*- or HPRT (hypoxanthine-guanine phosphoribosyl-transferase)–specific primers (*21*). (**B**) Pooled lymph node and spleen cells from BALB/c mice were sorted into the indicated compartments, and nonsaturating RT-PCR analyses were carried out. CD4$^+$ cells were further separated into CD25$^+$ or CD25$^-$ cells. (**C**) Quantification of relative *Foxp3* mRNA levels in indicated CD4$^+$ T cell subsets. cDNA samples were subjected to real-time quantitative PCR analyses using primers and an internal fluorescent probe specific for *Foxp3* or HPRT. The relative quantity of *Foxp3* in each sample was normalized to the relative quantity of HPRT (*21*). (**D**) CD25$^-$CD4$^+$ (open symbols) or CD25$^+$CD4$^+$ cells (closed symbols) were activated for indicated hours with plate-bound CD3 mAb in the presence of IL-2 (circles) or CD28 mAb (squares) and assessed for the expression of *Foxp3* by real-time quantitative RT-PCR. (A) to (D) each show one representative result of three independent experiments.

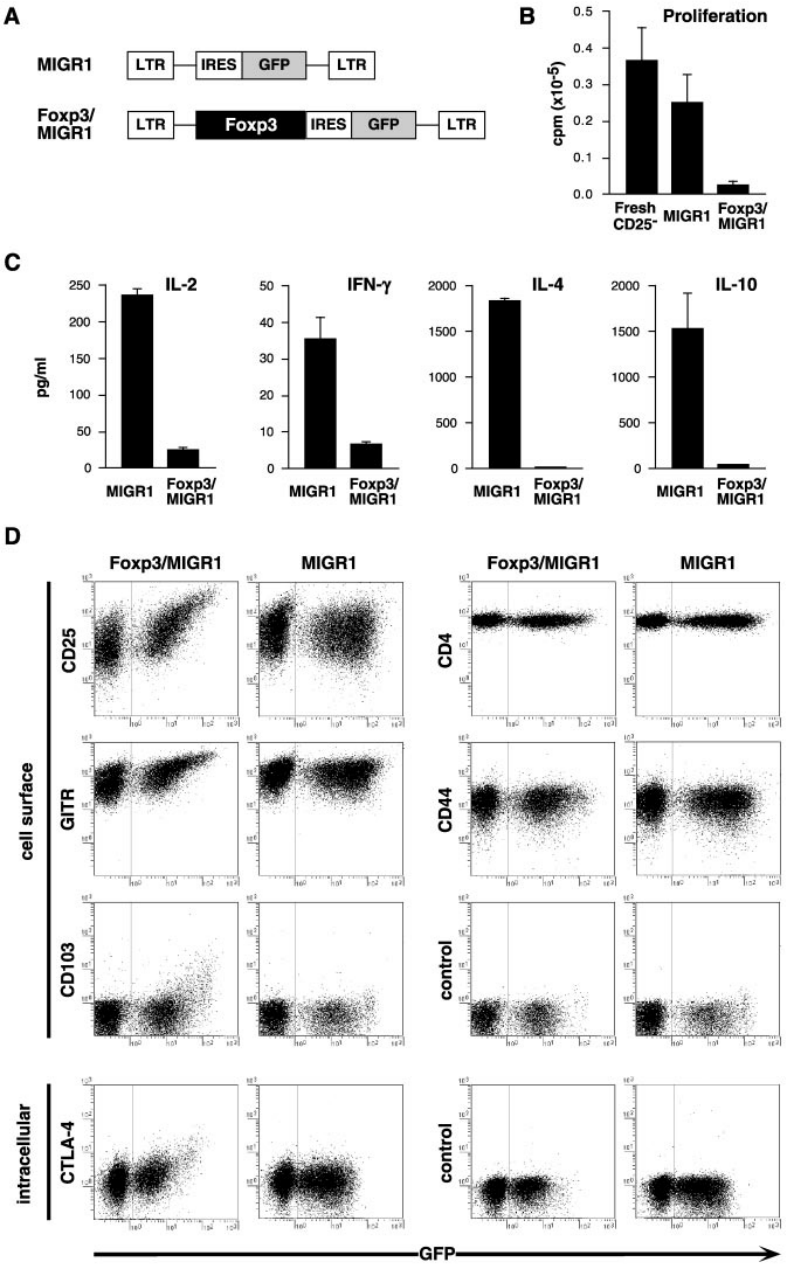

Fig. 2. Retroviral transduction of *Foxp3* into naïve $CD4^+$ T cells. (**A**) *Foxp3* cDNA was inserted into the MIGR1 retrovirus vector (*21*). This vector simultaneously expresses two cDNAs, *Foxp3* and GFP, with the use of an internal ribosomal entry site (IRES). (**B**) CD3 mAb–stimulated proliferative response of freshly isolated $CD25^-CD4^+$ cells and GFP^+ Foxp3/MIGR1- or MIGR1-infected $CD25^-CD4^+$ cells. [^{3}H] thymidine incorporation was measured as an indicator of cell proliferation and expressed as the mean (± SD) of triplicate cultures. cpm, counts per minute. (**C**) IL-2, IFN-γ, IL-4, or IL-10 concentration in the culture supernatant of CD3 mAb–stimulated culture of GFP^+ Foxp3/MIGR1- or MIGR1-infected $CD25^-CD4^+$ cells (mean ± SD). (**D**) Foxp3/MIGR1- or MIGR1-infected T cells derived from $CD25^-CD4^+$ cells were stained with phycoerythrin (PE)–labeled mAb for CD25, GITR, CD103, CD4, CD44, or an irrelevant antigen (control), along with detection of GFP. Intracellular CTLA-4 molecules were detected with PE-labeled CTLA-4 or isotype-matched control mAb (*21*). (B) to (D) each show one representative result of three independent experiments.

scurfy, also succumbs to similar X-linked recessive autoimmune and inflammatory diseases as a result of uncontrolled activation and expansion of $CD4^+$ T cells (*13*–*16*). Recent efforts to identify the genetic defect in IPEX/XLAAD patients or scurfy mice have revealed mutations in a common gene, *Foxp3*, which encodes a forkhead-winged–helix transcription factor designated Scurfin (*17*–*20*). Immunological similarities between the autoimmunity and inflammation produced by manipulating $CD25^+CD4^+$ T_R cells and those induced by genetic defects in *Foxp3* prompted us to investigate the possible contribution of *Foxp3* to the development or function of regulatory T cells.

We first examined the expression of *Foxp3* mRNA in the thymus and the periphery of normal mice by reverse transcriptase–polymerase chain reaction (RT-PCR) (*21*). In the thymus, $CD25^+CD4^+CD8^-$ thymocytes, which constitute 5% of $CD4^+CD8^-$ thymocytes (*7*), predominantly transcribed *Foxp3*, whereas $CD4^-CD8^+$ and other immature thymocyte populations did not (Fig. 1A). In the periphery, $CD4^+$ T cells specifically transcribed the gene, whereas $CD8^+$ T cells and $CD19^+$ B cells did not (Fig. 1B) (*17*). Among $CD4^+$ T cells, the $CD25^+$ subset, which constitutes 5 to 10% of $CD4^+$ T cells in normal naïve mice, exhibited predominant transcription. Real-time quantitative PCR analyses revealed that the *Foxp3* mRNA level in $CD25^+CD4^+$ cells was 100-fold more abundant than in $CD25^-CD4^+$ cells (Fig. 1C). A low level of expression in $CD25^-CD4^+$ cells was confined to the $CD45RB^{low}$ population, which has been previously reported to contain regulatory activity (*22*, *23*). These results indicate that *Foxp3* expression is predominantly restricted to the $CD25^+CD4^+$ population in both the thymus and periphery.

Expression of *Foxp3* is not a mere consequence of T cell activation, because in vitro stimulation of $CD25^-CD4^+$ cells for 3 days by monoclonal antibodies (mAbs) to CD3 in the presence of IL-2 or CD28 mAb failed to elicit *Foxp3* expression (Fig. 1D). Neither effector Th1 nor effector Th2 cells prepared from naïve T cells expressed *Foxp3* (fig. S1). Furthermore, stimulation of $CD25^+CD4^+$ cells with CD3 mAb and IL-2 did not alter their expression levels of *Foxp3*. Thus, *Foxp3* expression is stable in $CD25^+CD4^+$ T_R cells irrespective of the mode or state of activation.

We next determined whether forced expression of *Foxp3* in naïve T cells could convert these cells toward a regulatory T cell phenotype. Bicistronic retroviral vectors expressing *Foxp3* and green fluorescent protein (GFP) (Foxp3/MIGR1) or GFP alone (MIGR1) were generated (Fig. 2A). Peripheral $CD25^-CD4^+$ cells from normal naïve mice were stimulated with CD3 mAb and IL-2 and infected with either retrovirus. One week after infection, the proliferative re-

sponses of GFP$^+$ cells to T cell receptor (TCR) stimulation, cytokine production, and expression of cell surface molecules were examined. Retroviral transduction led to expression of GFP in 30 to 60% of CD4$^+$ cells. Upon TCR stimulation with CD3 mAb, GFP$^+$ cells from Foxp3/MIGR1-infected cultures proliferated poorly in contrast to the vigorous proliferation of GFP$^+$ cells from control MIGR1-infected cells or freshly prepared CD25$^-$CD4$^+$ cells (Fig. 2B). In addition, Foxp3/MIGR1-infected GFP$^+$ cells produced very little but detectable IL-2, IFN-γ, IL-4, and IL-10 as compared to GFP$^+$ MIGR1-infected cells, which secreted large amounts of these cytokines (Fig. 2C). Although these *Foxp3*-expressing cells produced higher amounts of cytokines than freshly isolated CD25$^+$CD4$^+$ cells (fig. S2), cytokine-producing cells were largely confined to cells expressing low levels of GFP (and hence *Foxp3*).

Naturally arising CD25$^+$CD4$^+$ T_R cells characteristically express CD25, cytotoxic T lymphocyte-associated antigen–4 (CTLA-4), glucocorticoid-induced tumor necrosis factor receptor family–related gene (GITR), and CD103 (α_E integrin) (*6*–*10*, *24*–*28*). Although the activation of CD25$^-$CD4$^+$ cells for retroviral infection led to expression of these molecules in both Foxp3/MIGR1- and MIGR1-infected cells, GFP$^+$ cells in the former expressed CD25, GITR, and CTLA-4 at higher levels than GFP$^-$ cells or GFP$^+$ MIGR1-infected cells (Fig. 2D, table S1). Among the GFP$^+$ *Foxp3*-transduced cells, the higher the level of GFP (*Foxp3*) expression, the higher the expression was of these molecules (Fig. 2D). Furthermore, only GFP^{high} (*Foxp3*^{high}) cells in the Foxp3/MIGR1-infected cells expressed CD103, with no expression on MIGR1-infected cells. Because *Foxp3* transduction did not affect the expression levels of either CD4 or CD44, the *Foxp3*-induced high expression of these T_R-associated molecules is most likely due to specific genetic instruction and not simply excessive cell activation by *Foxp3*. From these experiments, we conclude that transduction of *Foxp3* could render naïve T cells hyporesponsive to TCR stimulation, inhibit cytokine production, and up-regulate expression of cell surface molecules closely associated with the regulatory function of naturally occurring CD25$^+$CD4$^+$ T_R cells (*29*, *30*).

We next assessed the potential of *Foxp3*-transduced T cells to show suppressive activity. Foxp3/MIGR1-infected CD25$^-$CD4$^+$ T cells could specifically reduce proliferation of freshly prepared CD25$^-$CD4$^+$ responder T cells when stimulated with CD3 mAb (Fig. 3A). This suppression was associated with the inhibition of IL-2 production of the responder population in a fashion similar to that of natural CD25$^+$CD4$^+$ T_R cells (Fig. 3B) and correlated with the level of GFP (*Foxp3*) expression in the infected population [Supporting Online Material (SOM) Text, fig. S3A]. These GFP^{high} cells also suppressed IL-4 secretion by CD25$^-$CD4$^+$ responder T cells (fig. S3B). CD25$^+$CD4$^+$ cells, whether infected with Foxp3/MIGR1 or MIGR1, showed equally potent suppressive activity (Fig. 3A).

To examine whether antigen-specific naïve T cells could be converted to regulatory T cells by ectopic *Foxp3* expression, we used recombination-activating gene (RAG)–deficient DO11.10 CD4$^+$ T cells, which express ovalbumin (OVA) peptide–specific trans-

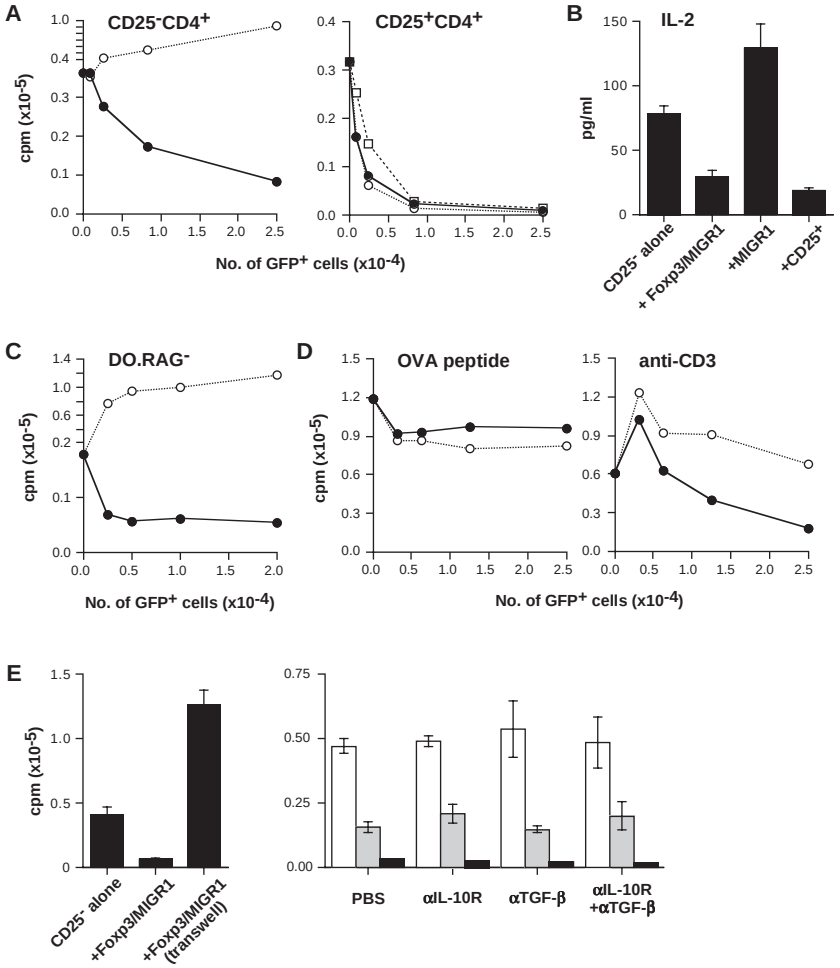

Fig. 3. Suppressive activity of *Foxp3*-transduced naïve CD4$^+$ T cells. (**A**) Graded doses of GFP$^+$ cells infected with either Foxp3/MIGR1 (closed circles) or MIGR1 (open circles) derived from BALB/c CD25$^-$CD4$^+$ (left) or CD25$^+$CD4$^+$ cells (right) were cultured with 2.5 × 10^4 freshly prepared CD25$^-$CD4$^+$ cells for 72 hours with CD3 mAb and 5.0 × 10^4 antigen-presenting cells (APCs). Proliferation of cells was assessed as in Fig. 2B. Freshly isolated CD25$^+$CD4$^+$ cells were also included in the assay (open squares). (**B**) Freshly prepared CD25$^-$CD4$^+$ cells alone or mixed with the same number of GFP$^+$ Foxp3/MIGR1-(+Foxp3/MIGR1) or MIGR1-infected CD25$^-$CD4$^+$ cells (+MIGR1) or freshly isolated CD25$^+$CD4$^+$ cells (+CD25$^+$) were stimulated with CD3 mAb, and IL-2 concentration in the culture supernatant was measured as in Fig. 2C. (**C**) GFP$^+$ cells from DO11.10/RAG-2$^{-/-}$ CD4$^+$ cells infected with Foxp3/MIGR1 (closed circles) or MIGR1 (open circles) were cultured with 2.0 × 10^4 freshly prepared DO11.10 CD4$^+$ cells in the presence of OVA peptide and 4.0 × 10^4 APCs. (**D**) BALB/c CD25$^-$CD4$^+$ cells were transduced with *Foxp3* (closed circles) or GFP alone (open circles) and sorted for GFP. Indicated numbers of GFP$^+$ cells were mixed with 2.5 × 10^4 DO11.10 TCR transgenic CD4$^+$ cells and stimulated with either specific OVA peptide (left) or CD3 mAb (right). (**E**) GFP$^+$ Foxp3/MIGR1-infected T cells derived from BALB/c CD25$^-$CD4$^+$ cells and an equal number of freshly prepared CD25$^-$CD4$^+$ cells were separated or nonseparated by a semipermeable membrane and stimulated with CD3 mAb and APCs on each side (left). IL-10 receptor (IL-10R) mAb, TGF-β mAb, or the mixture of these two was added to the culture of freshly prepared CD25$^-$CD4$^+$ cells either alone (white bars) or in the presence of GFP$^+$ Foxp3/MIGR1-infected CD25$^-$CD4$^+$ cells (gray bars) or freshly prepared CD25$^+$CD4$^+$ cells (black bars) (right) (*21*). (A) to (E) each show one representative result of three independent experiments.

genic TCRs, are deficient in natural $CD25^+CD4^+$ T_R cells (*7*), and scarcely express *Foxp3* (SOM Text, fig. S4). In the absence of specific antigen, almost all T cells from these animals remain in a naïve state. Transgenic $CD4^+$ T cells infected with Foxp3/MIGR1 suppressed the proliferation of freshly prepared noninfected transgenic T cells upon stimulation with specific OVA peptides, whereas those infected with MIGR1 did not (Fig. 3C). These results collectively indicate that ectopic expression of *Foxp3* was sufficient to convert otherwise nonregulatory naïve T cells toward a regulatory T cell phenotype capable of suppressing proliferation of other T cells, presumably through inhibition of IL-2 production (SOM Text, fig. S5).

Foxp3-transduced $CD4^+$ T cells appeared to exert the suppressive activity in a similar manner to that of naturally occurring $CD25^+CD4^+$ T_R cells (SOM Text, fig. S6). First, *Foxp3*-transduced cells derived from BALB/c $CD25^-CD4^+$ cells failed to suppress the proliferative response of DO11.10 TCR transgenic $CD4^+$ T cells when stimulated with OVA peptide, whereas polyclonal stimulation with CD3 mAb induced suppression (Fig. 3D). This indicates that *Foxp3*-transduced T cells require stimulation through TCRs to exert suppression (*29*, *30*). Second, *Foxp3*-infected T cells failed to suppress other T cells when separated by a semipermeable membrane, in contrast to effective suppression that was observed when cell-cell contact was allowed (Fig. 3E). These separated *Foxp3*-infected T cells even enhanced T cell responses across the membrane, presumably via cytokines they produced (fig. S2). In addition, neutralization of transforming growth factor–β (TGF-β) or blocking of IL-10 receptor, either alone or in combination, failed to abrogate suppression, as was the case with natural $CD25^+CD4^+$ T_R cells. These results indicate that in vitro suppression by *Foxp3*-transduced T cells may not be mediated by humoral factors but requires cell contact (*29*, *30*).

Finally, we examined whether Foxp3/MIGR1-infected T cells could suppress in vivo the inflammation and the autoimmune disease that have been shown to develop in the absence of T cell regulation. For this, we used a model of IBD and autoimmune gastritis that can be induced in severe combined immunodeficiency (SCID) mice by the transfer of $CD25^-CD45RB^{high}CD4^+$ T cells from normal BALB/c mice and prevented by cotransfer of $CD25^+CD4^+$ T_R cells (*10*, *31*) (Fig. 4). $CD25^-CD45RB^{high}CD4^+$ cells from BALB/c mice were infected with Foxp3/MIGR1 or MIGR1, and GFP^+ cells were cotransferred with freshly prepared $CD25^-CD45RB^{high}CD4^+$ cells. The GFP^+ *Foxp3*-transduced cells inhibited weight loss, diarrhea, and histological development of colitis and gastritis induced by the transfer of $CD25^-CD45RB^{high}CD4^+$ cells as effectively as naturally occurring $CD25^+CD4^+$ cells. By contrast, the cells transduced with GFP alone failed to prevent disease, and rather enhanced weight loss and the development of colitis. Thus, transduction of *Foxp3* can render naïve T cells capable of preventing autoimmune gastritis and IBD caused by dysregulated immune responses toward gastric self-antigens and commensal bacteria, respectively (SOM Text).

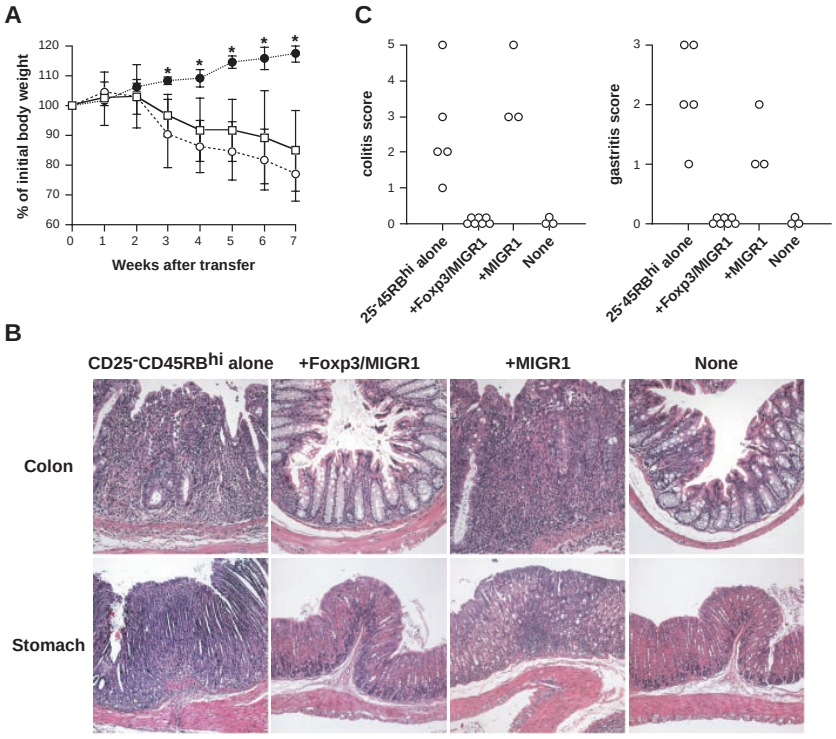

Fig. 4. Prevention of IBD and autoimmune gastritis by *Foxp3*-transduced T cells. (**A**) C.B-17 *scid* mice received 4×10^5 fresh $CD25^-CD45RB^{high}CD4^+$ cells either alone ($n = 6$, where n is the number of mice) (open squares) or together with 1.2×10^6 GFP^+ sorted cells derived from $CD25^-CD45RB^{high}CD4^+$ cells infected with Foxp3/MIGR1 ($n = 7$) (closed circles) or MIGR1 ($n = 5$) (open circles). Body weight is represented as the percentage of initial weight (mean ± SD). Astericks indicate significant difference, $P < 0.01$, Foxp3/MIGR1 versus other two groups by Mann-Whitney test. (**B**) Histopathology of the colon and stomach in each group and in an unreconstituted SCID mouse (None). (**C**) Colitis (left) and gastritis (right) were histologically scored. Two mice in the group cotransferred with MIGR1-infected cells and one transferred with $CD25^-CD45RB^{high}CD4^+$ cells alone died of debilitation before histological examination. Results shown in (A) to (C) are from a total of three independent experiments.

The present study shows that *Foxp3* is predominantly expressed in the $CD25^+CD4^+$ T_R population naturally arising in the thymus and periphery and that *Foxp3* expression in naïve T cells can convert these cells to a regulatory T cell phenotype functionally similar to naturally occurring $CD25^+CD4^+$ T_R cells. This result suggests that *Foxp3* may be a master regulatory gene for cell-lineage commitment or developmental differentiation of regulatory T cells in the thymus and the periphery. Our results also indicate that, in defining the naturally occurring $CD4^+$ regulatory T cells engaged in preventing autoimmune disease and immunopathology, *Foxp3* represents a more specific marker than currently used cell-surface molecules (such as CD25, CD45RB, CTLA-4, and GITR), which are unable to completely discriminate between regulatory T cells and activated, effector, or memory T cells.

Mutations in the *Foxp3* gene culminate in the development of a fatal lymphoproliferative disorder associated with multiorgan pathology both in mice and humans (*12–20*). *FOXP3* is predominantly expressed in human $CD25^+CD4^+$ T cells as well (*32*). Furthermore, transduction of a mutant *Foxp3* lacking the forkhead domain, similar to the mutated *Foxp3* in scurfy mice (*17*), failed to confer suppressive activity to $CD25^-CD4^+$ T cells (fig. S7). The present results therefore suggest that mutations of the *Foxp3* gene may cause these disorders through developmental or functional abnormality of the $CD25^+CD4^+$ T_R population.

Potentially, generation of T_R cells by *Foxp3* transduction of naïve T cells may provide a previously unstudied therapeutic mode for treatment of autoimmune and inflammatory diseases and in transplantation tolerance.

References and Notes

1. L. Van Parijs, A. K. Abbas, *Science* **280**, 243 (1998).
2. S. Sakaguchi, *Cell* **101**, 455 (2000).
3. K. J. Maloy, F. Powrie, *Nature Immunol.* **2**, 816 (2001).
4. A. Coutinho, S. Hori, T. Carvalho, I. Caramalho, J. Demengeot, *Immunol. Rev.* **182**, 89 (2001).
5. E. M. Shevach, *Nature Rev. Immunol.* **2**, 389 (2002).
6. S. Sakaguchi, N. Sakaguchi, M. Asano, M. Itoh, M. Toda, *J. Immunol.* **155**, 1151 (1995).
7. M. Itoh *et al.*, *J. Immunol.* **162**, 5317 (1999).
8. M. Asano, M. Toda, N. Sakaguchi, S. Sakaguchi, *J. Exp. Med.* **184**, 387 (1996).
9. E. Suri-Payer, A. Z. Amar, A. M. Thornton, E. M. Shevach, *J. Immunol.* **160**, 1212 (1998).
10. S. Read, V. Malmstrom, F. Powrie, *J. Exp. Med.* **192**, 295 (2000).
11. M. A. Curotto de Lafaille *et al.*, *J. Exp. Med.* **194**, 1349 (2001).
12. R. S. Wildin, S. Smyk-Pearson, A. H. Filipovich, *J. Med. Genet.* **39**, 537 (2002).
13. V. L. Godfrey, J. E. Wilkinson, L. B. Russell, *Am. J. Pathol.* **138**, 1379 (1991).
14. P. J. Blair *et al.*, *J. Immunol.* **153**, 3764 (1994).
15. L. B. Clark *et al.*, *J. Immunol.* **162**, 2546 (1999).
16. J. L. Zahorsky-Reeves, J. E. Wilkinson, *Eur. J. Immunol.* **31**, 196 (2001).
17. M. E. Brunkow *et al.*, *Nature Genet.* **27**, 68 (2001).
18. T. A. Chatila *et al.*, *J. Clin. Investig.* **106**, R75 (2000).
19. R. S. Wildin *et al.*, *Nature Genet.* **27**, 18 (2001).
20. C. L. Bennett *et al.*, *Nature Genet.* **27**, 20 (2001).
21. Materials and methods are available as supporting material on *Science* Online.
22. L. A. Stephens, D. Mason, *J. Immunol.* **165**, 3105 (2000).
23. O. Annacker *et al.*, *J. Immunol.* **166**, 3008 (2001).
24. T. Takahashi *et al.*, *J. Exp. Med.* **192**, 303 (2000).
25. B. Salomon *et al.*, *Immunity* **12**, 431 (2000).
26. J. Shimizu, S. Yamazaki, T. Takahashi, Y. Ishida, S. Sakaguchi, *Nature Immunol.* **3**, 135 (2002).
27. R. S. McHugh *et al.*, *Immunity* **16**, 311 (2002).
28. J. Lehmann *et al.*, *Proc. Natl. Acad. Sci. U.S.A.* **99**, 13031 (2002).
29. T. Takahashi *et al.*, *Int. Immunol.* **10**, 1969 (1998).
30. A. M. Thornton, E. M. Shevach, *J. Exp. Med.* **188**, 287 (1998).
31. E. Suri-Payer, H. Cantor, *J. Autoimmun.* **16**, 115 (2001).
32. S. Hori, T. Nomura, S. Sakaguchi, unpublished data.

33. We thank K. J. Wood, Z. Fehervari, and T. Takahashi for critically reading the manuscript; W. S. Pear and T. Kitamura for reagents; and T. Matsushita for histology. Supported by grants-in-aid from the Ministry of Education, Sports and Culture, the Ministry of Human Welfare, and the Organization for Pharmaceutical Safety and Research of Japan.

Supporting Online Material

www.sciencemag.org/cgi/content/full/1079490/DC1
Materials and Methods
SOM Text
Figs. S1 to S7
Table S1
References

17 October 2002; accepted 23 December 2002
Published online 9 January 2003;
10.1126/science.1079490
Include this information when citing this paper.

Rewiring MAP Kinase Pathways Using Alternative Scaffold Assembly Mechanisms

Sang-Hyun Park, Ali Zarrinpar, Wendell A. Lim*

How scaffold proteins control information flow in signaling pathways is poorly understood: Do they simply tether components, or do they precisely orient and activate them? We found that the yeast mitogen-activated protein (MAP) kinase scaffold Ste5 is tolerant to major stereochemical perturbations; heterologous protein interactions could functionally replace native kinase recruitment interactions, indicating that simple tethering is largely sufficient for scaffold-mediated signaling. Moreover, by engineering a scaffold that tethers a unique kinase set, we could create a synthetic MAP kinase pathway with non-natural input-output properties. These findings demonstrate that scaffolds are highly flexible organizing factors that can facilitate pathway evolution and engineering.

Scaffold proteins are known to play a critical role in a growing number of signaling pathways, including several mitogen-activated protein kinase (MAPK) cascades (*1–4*). In the budding yeast *Saccharomyces cerevisiae*, the scaffold proteins Ste5 and Pbs2 are essential for the mating and high–osmolarity response MAPK pathways, respectively (*5–8*). These scaffold proteins contain binding sites for each of the pathway kinases, as well as for upstream signaling input proteins (Fig. 1).

Despite their importance, little is known about the mechanism by which scaffold proteins such as Ste5 contribute to efficient and specific signaling (*9*). One model is that scaffold proteins simply tether pathway components, increasing their likelihood of acting on one another. However, one might expect a simple tethering scaffold to enhance but not be required for signaling. Thus, because Ste5 is essential for signaling, and because of evidence supporting conformational changes induced by scaffold-kinase association (*10, 11*), an alternative model is that Ste5 plays a more complex catalytic role, precisely orienting and/or allosterically regulating pathway kinases (*4*). One way to distinguish between these models would be to probe pathway sensitivity to perturbations in assembly mechanisms. If pathway function depended on precise catalytic participation of the scaffold, then strict stereochemical requirements for kinase recruitment would be expected.

We therefore tested whether non-native protein-protein interactions could be used to build a scaffolded assembly capable of mediating proper mating pathway connectivity and function. We took advantage of several known mutations in Ste5 that selectively destroy recruitment of the MAPK kinase kinase (MAPKKK) Ste11 and the MAPK kinase (MAPKK) Ste7. These mutations, respectively termed Ste5* and Ste5**, each resulted in a nonfunctional mating pathway (*12*). Defective recruitment interactions were then replaced with a heterologous protein-protein interaction (Fig. 2A): the well-characterized heterodimerization interaction between PDZ domains from the mammalian proteins neuronal nitric oxide synthase (nNOS) and syntrophin (*13, 14*). PDZ domains are interaction modules involved in assembly of diverse signaling complexes in higher eukaryotes (*15,*

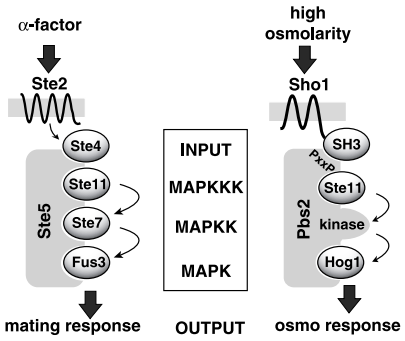

Fig. 1. Yeast mating and high-osmolarity MAPK pathways require scaffold proteins Ste5 and Pbs2. Both pathways require the shared MAPKKK Ste11 but exhibit no cross-signaling under normal conditions. Ste5 has distinct docking sites for Ste11, the MAPKK Ste7, and the MAPK Fus3 (or the partially redundant MAPK Kss1, not shown for simplicity) (*5–7*). Input to Ste5 occurs through a docking site for Ste4, the G_β subunit of the heterotrimeric guanine nucleotide–binding protein activated upon pheromone binding to the α-factor receptor, Ste2. Pbs2 functions as both the scaffold and MAPKK of the osmolarity pathway: It has a MAPKK domain, and it has been shown to bind Ste11 and the MAPK Hog1 (precise binding sites have not been identified) (*8*). Pbs2 also binds the Src homology 3 (SH3) domain from the upstream osmosensor Sho1 through a proline-rich docking site (residues 94 to 100), indicated by PxxP (*26*). A second branch of the osmoresponse pathway involving the two-component sensor protein Sln1 has been omitted for simplicity (*27*). This branch of the pathway does not require Sho1 or Ste11. All of the studies described here were performed with strains lacking this pathway branch (*ssk2*Δ and *ssk22*Δ).

Department of Cellular and Molecular Pharmacology and Department of Biochemistry and Biophysics, University of California, 513 Parnassus Avenue, San Francisco, CA 94143, USA.

*To whom correspondence should be addressed. E-mail: wlim@itsa.ucsf.edu

DOCKET ALARM

Explore Litigation Insights

Docket Alarm provides insights to develop a more informed litigation strategy and the peace of mind of knowing you're on top of things.

Real-Time Litigation Alerts

Keep your litigation team up-to-date with **real-time alerts** and advanced team management tools built for the enterprise, all while greatly reducing PACER spend.

Our comprehensive service means we can handle Federal, State, and Administrative courts across the country.

Advanced Docket Research

With over 230 million records, Docket Alarm's cloud-native docket research platform finds what other services can't. Coverage includes Federal, State, plus PTAB, TTAB, ITC and NLRB decisions, all in one place.

Identify arguments that have been successful in the past with full text, pinpoint searching. Link to case law cited within any court document via Fastcase.

Analytics At Your Fingertips

Learn what happened the last time a particular judge, opposing counsel or company faced cases similar to yours.

Advanced out-of-the-box PTAB and TTAB analytics are always at your fingertips.

API

Docket Alarm offers a powerful API (application programming interface) to developers that want to integrate case filings into their apps.

LAW FIRMS
Build custom dashboards for your attorneys and clients with live data direct from the court.

Automate many repetitive legal tasks like conflict checks, document management, and marketing.

FINANCIAL INSTITUTIONS
Litigation and bankruptcy checks for companies and debtors.

E-DISCOVERY AND LEGAL VENDORS
Sync your system to PACER to automate legal marketing.